SUPPLEMENTARY INFORMATION

doi:10.1038/nature10971

S1 MODEL DESCRIPTION

We consider an individual-based model with discrete non-overlapping generations in one- or two-dimensional continuous space with wrap-around boundaries. Below, we describe the two-dimensional model, from which the corresponding one-dimensional model is readily generated by removing the spatial y-dimension. Each individual has a spatial location and is characterized by a display trait (expressed only in males) and a preference trait (expressed only in females). In our main set of model runs, these traits are assumed to be governed by separate unlinked haploid loci, each with two alleles (display alleles are denoted by Q/q and preference alleles by P/p). Each generation, N individuals are produced and compete for resources, with those experiencing stronger competition being more likely to die before reaching reproductive maturity. Resources in our model may be interpreted in the broadest possible sense, describing the biotic and abiotic factors that are subject to local ecological competition. Among the individuals surviving ecological competition, females choose mates, with the probability of a specific male being chosen depending on her mating preference and the spatial distance separating them. Females produce offspring in proportion to their fecundities. Offspring then disperse from their natal location and the parents die. Below we detail these steps in the order in which they occur. The names and descriptions of parameters and variables are listed in Table S1.

S1.1 Competition for resources

The habitat at each location (x, y) is characterized by the local density $k(x, y)$ of available resources. The total amount of resources over the spatial arena is given by $K = \iint k(x, y)\,\mathrm{d}x\,\mathrm{d}y$. The function relating resource gain to survival is chosen such that if every individual received an equal share of these resources, the expected number of survivors would be K. Consequently, we refer to $k(x, y)$ as the local carrying capacity and to K as the total carrying capacity. Except for Figs. 4 and S7, we investigate a local carrying capacity that is symmetrically bimodal, with two peaks located at $(x, y) = (0.25, 0.25)$ and $(x, y) = (0.75, 0.25)$. If constructed simply by summing two Gaussians centred at these peaks, resource availability would not be symmetric about the peaks. To avoid such an asymmetry, we construct a periodic landscape given by

$$k(x,y) = \left(b + \sum_{i,j} \exp\left(-\frac{(x-(0.25+i/2))^2 + (y-(0.25+j/2))^2}{2\sigma_k^2}\right)\right) k_0 \quad , \tag{1}$$

for x in $[0, 1]$ and y in $[0, 0.5]$, where the sum is taken over all pairs of integers, and where σ_k denotes the widths of the Gaussian peaks. The parameters b and k_0 allow us to adjust the average height and degree of variation in $k(x, y)$. Specifically, the height is adjusted such that the total carrying capacity equals K, and the degree of variation is adjusted to give the desired relation between peaks and troughs. For the local carrying capacity in Eq. 1, it is natural, for easy comparison between the one-dimensional and the two-dimensional model, to measure the degree of spatial variation along the transect spanning both peaks as

$$v = \frac{\max k(x,y) - \min k(x,y)}{\min k(x,y)} \, . \tag{2}$$

A value of $v = 0.25$ therefore means that the local carrying capacity is 25% higher at the peaks than at the troughs between them.

Table S1 | Model parameters and model variables

Symbol	Eq.	Description
Model parameters		
a		Strength of selection against Q-bearing males (only S2.10)
$k(x, y)$	1	Local carrying capacity at location (x, y)
l	12	Strength of mating-dependence in male dispersal (only S2.1)
m	11	Strength of mate-search costs
$s_{\max}$	6	Maximum survival probability
v	2	Spatial variation in local carrying capacity
K		Total carrying capacity
N		Number of offspring
α	8	Strength of female preference
$f_{\max}$	9	Maximum female fecundity
λ	13	Strength of density-dependent competition
σ_f	7	Width of female-preference distribution
σ_k	1	Width of peaks in local carrying capacity
σ_m		Width of movement distribution
σ_o		Width of offspring distribution (only S2.9)
σ_p	14	Width of female preference (only S2.9)
σ_s	4	Width of competition distribution
Model variables		
c_i	11	Mate-search costs of female i
d_{ij}	4	Spatial distance between individuals i and j
e_{ij}	7	Propensity for female i to encounter male j
f_i	9	Fecundity of female i
n_{ij}	4	Competitive effect of individual j on individual i
p_{ij}	8	Propensity for female i to choose male j as a mate
s_i	6	Survival probability of individual i
μ_i	10	Local density of preferred males as seen by female i
ρ_i	3	Resource share of individual i

For Fig. S7, landscapes are generated in a similar way, except that the heights and widths of the two peaks differ. For Fig. 4, the landscape is generated by adding white noise to the baseline level, filtered to have a reasonable amount of spatial autocorrelation, with the highest peak set to twice the height of the lowest trough.

Through competition, each individual obtains a share of the local carrying capacity, which we refer to as its resource share,

$$\rho_i = \frac{k(x_i, y_i)}{\sum_j n_{ij}} \, , \tag{3}$$

where n_{ij} is the contribution of individual j to the effective density of competitors at the location of individual i, and the sum extends over all N individuals. The competitive impact of individual j on individual i decreases with the distance d_{ij} separating them, according to a Gaussian function with standard deviation σ_s,

$$n_{ij} = \exp(-d_{ij}^2/(2\sigma_s^2))/(2\pi\sigma_s^2) \, ; \tag{4}$$

in the one-dimensional model, the divisor is $\sqrt{2\pi}\sigma_s$. Note that the effect n_{ii} of an individual i on itself declines as σ_s increases, because the individual then competes for resources over larger distances and thus has less of a negative impact on its available resources.

As defined, the resource share of an individual i is typically near K/N. This can be seen by assuming that the N individuals in the population are distributed over the arena according to the local carrying capacity, so that their expected density is $N\,k(x, y)/K$.

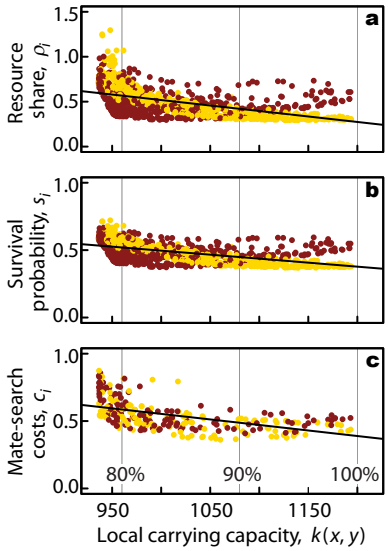

Figure S1 | Variation in three components of fitness as a function of the local carrying capacity experienced by each individual at $t = 1000$ for the model run in Fig. 1d. Individuals are coloured according to their genotype at the display locus. **a,** Resource share ρ_i in males and females. **b,** Survival probability s_i of males and females. **c,** Mate-search costs c_i of females that survive competition. Thick lines show least-squares linear regressions.

Replacing the sum over individuals in Eq. 3 with an integral over space, we obtain

$$\rho_i = \frac{k(x_i, y_i)}{\iint \frac{N\,k(x,y)}{K} \frac{\exp(-((x_i-x)^2+(y_i-y)^2)/(2\sigma_s^2))}{2\pi\sigma_s^2}\,\mathrm{d}x\,\mathrm{d}y} \qquad (5)$$
$$= K/N + O(v)\,,$$

where the second line assumes that spatial variation in the local carrying capacity is low. In our individual-based model runs, departures from the above occur due to clumping, fecundity variation over space (Section S1.4), as well as discrepancies due to replacing the sum in Eq. 3 with the integral in Eq. 5 (especially when σ_s is very small or large relative to the arena). That said, the mean resource share is typically close to K/N in our model runs.

In Fig. S1 we show the effect of spatial variation in local carrying capacity $k(x_i, y_i)$ on various components of fitness, including the resource share ρ_i. Interestingly, ecological competition is weaker (ρ_i is higher) in regions of low carrying capacity (Fig. S1a), increasing the survival probability s_i of individuals in these regions (Section S1.2 and Fig. S1b). This occurs because females are less likely to encounter preferred males wherever the carrying capacity is low, causing their fecundity to be lower due to increased mate-search costs c_i (Section S1.4 and Fig. S1c). Consequently, fewer offspring are produced than expected based on the low local carrying capacity, resulting in weaker competition among those offspring. The net result of lower ecological competition and higher mate-search costs in regions with low local carrying capacity is that females have roughly equal fitness across space.

S1.2 Survival

We assume that individuals that gain more resources are more likely to survive to reproductive maturity. The probability s_i of such survival is assumed to be zero when an individual fails to gain any resources, to rise approximately linearly with its resource share ρ_i when that share is small, and to taper off at a maximum survival probability of $s_{\max}$ (ranging between 0 and 1). Specifically, we use a hyperbolic (or Holling type-2) function[27] to relate resource share to the probability of survival,

$$s_i = \frac{s_{\max}}{1 + r/\rho_i}\,, \qquad (6)$$

where r is the resource share that must be obtained for an individual to survive with a probability equal to half the maximum survival probability. Unless stated otherwise, we assume that the maximum probability $s_{\max}$ of surviving to reproductive maturity equals 1.

The value of r is chosen to ensure that, on average, K individuals survive to reproduce if all individuals obtain an equal share of resources ($\rho_i = K/N$). By setting the expected survival probability s_i to K/N in Eq. 6 and substituting $\rho_i = K/N$, we obtain $r = s_{\max} - K/N$. With this choice of r, approximately K individuals survive each generation (with a variance that is typically small). For example, in Fig. S1, the average survival probability is 0.484, close to the expected value of $K/N = 0.5$. While competition for resources causes substantial mortality, survival probabilities across the arena differ only slightly (Fig. S1b). Importantly, the survival of an individual does not depend on whether or not it is a hybrid.

S1.3 Mating

Of the individuals that survive to mate, the probability that female i chooses male j as a mate depends on whether his display trait matches her preference trait and on the spatial distance separating them. Females bearing a P (p) allele prefer males bearing a Q (q) allele by a factor α. We assume that females encounter males in the vicinity of their home location. Specifically, each female spends a proportion of time at distance d_{ij} from her home that is described by a Gaussian distribution with standard deviation σ_f, so that her encounter probability e_{ij} with a male at distance d_{ij} is proportional to

$$e_{ij} = \exp(-d_{ij}^2/(2\sigma_f^2))/(2\pi\sigma_f^2)\,; \qquad (7)$$

in the one-dimensional model, the divisor is $\sqrt{2\pi}\sigma_f$. In our main model, we assume that females encounter resources and males over the same spatial scales (i.e., $\sigma_f = \sigma_s$); we relax this assumption in Fig. S6. The probability that female i chooses male j as a mate is proportional to

$$p_{ij} = \alpha^{\delta_{ij}-1} e_{ij}\,, \qquad (8)$$

where δ_{ij} equals 1 when the display trait of male j matches the preference trait of female i, and 0 otherwise. Once a female chooses a mate, we assume that all her offspring are sired by that male (monogamy).

S1.4 Reproduction

The fecundity of a female i is given by

$$f_i = f_{\max}(1 - c_i)\,, \qquad (9)$$

where $f_{\max}$ is the maximum fecundity and c_i (ranging from 0 to 1) measures the cost associated with finding a preferred mate for female i. The factor $1 - c_i$ is assumed to be zero when there are no preferred males locally, to rise approximately linearly with the local density of preferred males,

$$\mu_i = \sum_{\text{males } j} p_{ij}\,, \qquad (10)$$

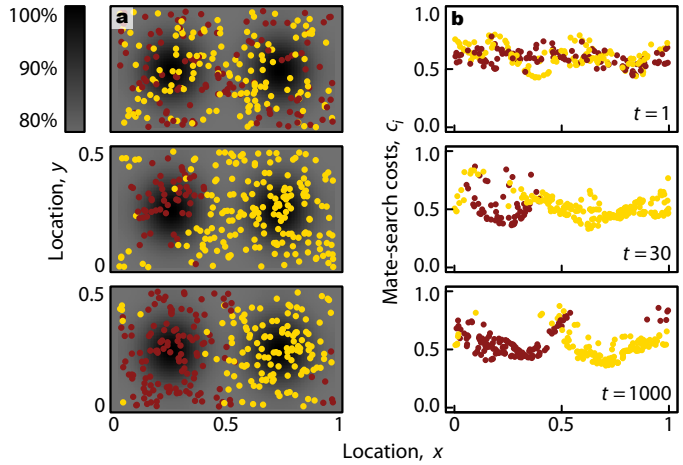

Figure S2 | Mate-search costs for the model run in Fig. 1d. Panels in column **a** are identical to those in Fig. 1d, except that only females are shown and they are coloured according to their preference allele. Panels in column **b** show the costs associated with searching for a mate and rejecting non-preferred males for each female (Eq. 9), as a function of her location y. Here, with $m/K = 1$, female fecundity is typically only halved by mate-search costs.

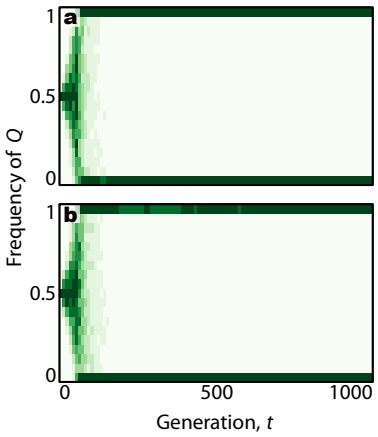

Figure S3 | Effects of mating-dependent dispersal in males. Panels show distributions of allele frequencies at the display locus through time across 1000 replicate model runs in a two-dimensional landscape with a uniform local carrying capacity; coexistence occurs only when these frequencies remain intermediate. Darker shading indicates a higher probability of observing a given frequency of the Q allele. Panel **a** is identical to Fig. 2b. Panel **b** is the same as **a**, except with mating-dependent dispersal in males ($l = 100$). Results for other values of l are qualitatively identical. Model runs are initialized as in Fig. 2. All other parameters are as in Fig. 1b.

and to taper off at 1 when preferred mates are readily encountered, resulting in maximal fecundity. Specifically, we use a hyperbolic (or Holling type-2) function[28],

$$1 - c_i = \frac{1}{1 + m/\mu_i}\,, \tag{11}$$

where m is the value of μ_i at which a female's fecundity is halved by mate-search costs. Because μ_i is obtained by summing over the entire male population, its value can be large, on the order of the number of surviving males, so values of m on the order of the surviving population's size K are needed for costs to be appreciable. This is why we express m relative to K, specifying the ratio m/K in the figures. We refer to c_i as the mate-search cost of female i and to m as the strength of mate-search costs.

Unless noted otherwise, we use $m = 500$. In our main set of model runs (with $m/K = 1$), mate-search costs reduce female fecundity by about 50%, on average, from the maximum fecundity (Fig. S1c), with relatively minor differences in fecundity among females over space. Other values of m are explored in Fig. 3. For $m = 0$, all females have equal and maximal fecundity. As m is raised, fecundity declines and becomes more variable, with females in low-density regions or surrounded by non-preferred males having lower fecundity (Fig. S2).

After mating, offspring are produced. Inheritance at both loci is Mendelian, and we assume no linkage between the display and preference loci, except where noted (Section S2.9). To allow us to explore various parameters relating to competition and mate-search costs independently, we hold the total number of offspring constant at N. For each offspring, a mother is chosen in proportion to the females' fecundities. Consequently, the maximum fecundity $f_{\max}$ only matters insofar as it is high enough to result in at least N offspring being produced across the population. Similar patterns are observed when $f_{\max}$ is fixed and offspring numbers are given by a Poisson distribution with a mean of f_i for each female (data not shown). We consider N to be the total number of offspring surviving the phase during which resources are largely provided by the parents, after which the offspring move and begin the next phase of competition for resources.

S1.5 Movement

Each offspring moves from its mother's location according to a distance drawn from a Gaussian function with mean 0 and standard deviation σ_m. Movements occur in all directions with equal probability.

S2 MODEL EXTENSIONS

To assess the robustness of our results, we consider several extensions and/or modifications to our main model described above.

S2.1 Allowing mating to impact dispersal

To compare our results with those of Payne and Krakauer[16], we consider mating-dependent dispersal. In their model, male movement distances are lower for males with better mating prospects, and we thus assume that the movement distance of male j is drawn from a Gaussian function with mean 0 and standard deviation

$$\sigma_{m,j} = \sigma_m \exp\left(- l \frac{\sum_i p_{ij}}{\sum_{i,k} p_{ik}} \right), \tag{12}$$

where l determines how quickly movement distances decrease with increasing mating prospects and p_{ij} is given by Eq. 8 in Section S1.3. For $l = 0$, the above reduces to our main model. We find that the addition of mating-dependent dispersal in males extends coexistence times only marginally, if at all (compare Fig. S3a to S3b). We also examine the related case in which males with low mating prospects move farther, but again, coexistence times are not appreciably prolonged in our individual-based model.

S2.2 Introducing multiple allelic types

To examine whether long-term coexistence of more than two types is possible, we extend our main model so that one of n alleles $p_1, \ldots, p_n$ can occur at the preference locus and one of n alleles $q_1, \ldots, q_n$ can occur at the display locus. Specifically, in Fig. 4, we consider $n = 10$ preference and display types. A female with preference allele p_i prefers males with display allele q_i to all other males by the factor α. All other components of mate choice remain the same as for our main model with $n = 2$ mating types.

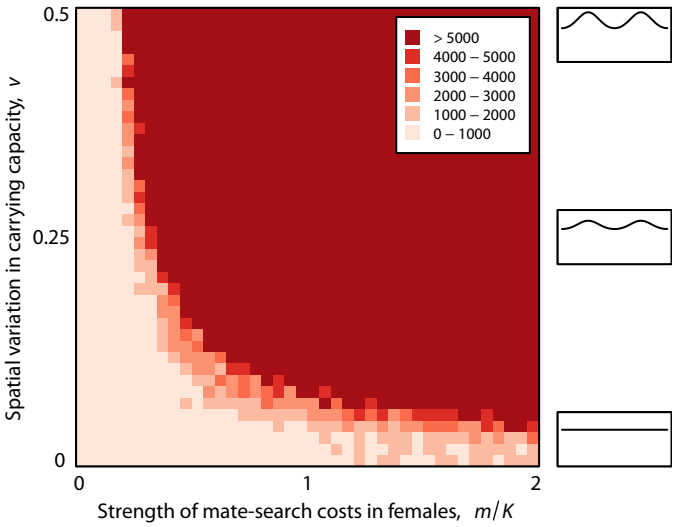

Figure S4 | Conditions for long-term coexistence with competition-dependent fecundity (Section S2.3) in a two-dimensional bimodal landscape. All parameters are as in Fig. 3.

S2.3 Allowing competition to impact fecundity

In our main model, competitive interactions reduce the survival probability of an individual. Alternatively, individuals that gain fewer resources might survive, but have lower fecundity. To explore this possibility, we allow all N offspring to survive, while reducing their reproductive success according to the impact of competition, as measured by s_i. Specifically, for males, the probability of being chosen as a mate is set to $p_{ij} = \alpha^{\delta_{ij}-1} e_{ij} s_i$. Likewise for females, fecundity is set to $f_i = f_{\max}(1 - c_i)s_i$. Such competition-dependent fecundity generates less demographic stochasticity, because all individuals reach reproductive maturity and can mate, albeit with reduced probability when their resource share ρ_i is low. Indeed, all else being equal, incorporating competitive effects on fecundity, rather than survival, enables long-term coexistence over a wider range of parameters (compare Fig. S4 to Fig. 3).

S2.4 Altering the strength of density-dependent competition

We define the strength of density-dependent competition as

$$\lambda = r/(1 - K/N), \tag{13}$$

with $r = s_{\max} - K/N$ (Section S1.2). In our main model, the maximum survival rate $s_{\max}$ is set to 1 so that $\lambda = 1$, indicating that survival is strongly density-dependent. At the other extreme, if $s_{\max}$ is set to K/N, all individuals survive with probability $s_{\max} = K/N$, regardless of their resource share, so there is no density-dependent effect on survival ($\lambda = 0$). As shown in Fig. S5b, coexistence does not occur in the absence of density dependence ($\lambda = 0$); spatial variation in local carrying capacity then becomes irrelevant and cannot stabilize mating domains in space. As the importance of competition increases (larger λ, or equivalently, larger $s_{\max}$), long-term coexistence can occur over a wider range of parameters. Once about half of the mortality is due to density-dependent competition ($\lambda > 0.5$), results become similar to those for $\lambda = 1$.

S2.5 Altering the impact of ecological competition

We explore the impact of ecological competition by varying the expected survival probability $\bar{s} = K/N$ of offspring, while the total carrying capacity K and the strength λ of density-dependent competition are held constant (Fig. S5c). When the impact of ecological competition is small ($\bar{s}$ near 1), long-term coexistence requires much higher levels of spatial variation in local carrying capacity.

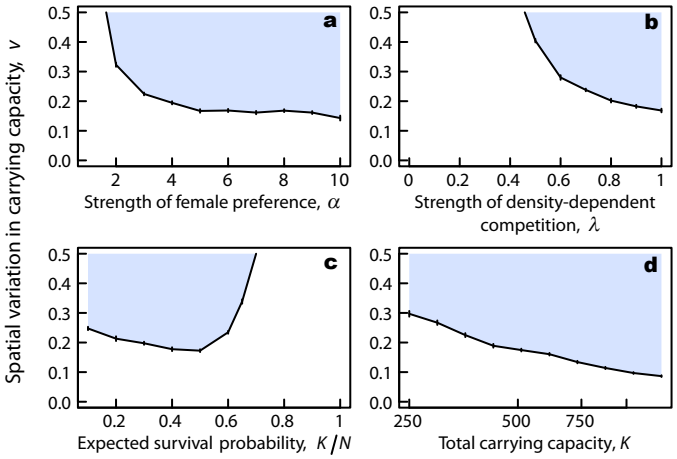

Figure S5 | Minimum level of spatial variation v in local carrying capacity needed to ensure long-term coexistence (shaded regions) in a two-dimensional bimodal landscape. The spatial variation v is increased until the average persistence time of 20 replicate runs exceeded $10K$ generations (vertical lines indicate standard errors). **a,** Effect of the strength α of female preference. Coexistence becomes more likely as female preferences become stronger (larger α), although once preference exceeds $\alpha \approx 5$, its impact is small. **b,** Effect of the strength λ of density-dependent competition (varying $s_{\max}$ while holding $K = 500$ and $N = 1000$ constant). The limit $\lambda = 0$ corresponds to completely density-independent survival, while the limit $\lambda = 1$ corresponds to completely density-dependent survival. **c,** Effect of the expected survival probability K/N (varying N while holding $K = 500$ and $\lambda = 1$ constant). Values near $K/N = 0$ correspond to very strong ecological competition, while the limit $K/N = 1$ corresponds to no ecological competition. **d,** Effect of the total carrying capacity K and $m/K = 1$ constant). All other parameters are as in Fig. 1d.

Once ecological competition is sufficiently strong (removing at least 40% of offspring; $\bar{s} < 0.6$), results become less sensitive to $\bar{s}$.

S2.6 Altering the degree of demographic stochasticity

If each of N offspring survives with probability $\bar{s}$, the number of mating individuals follows a binomial distribution with mean $N\bar{s}$ and variance $N\bar{s}(1 - \bar{s})$. The resultant coefficient of variation thus equals $\sqrt{1/\bar{s} - 1}/\sqrt{N}$, which grows as $\bar{s}$ shrinks. The associated rise in demographic stochasticity with smaller $\bar{s}$ may contribute to the slight rise in spatial variation in local carrying capacity required for maintaining long-term coexistence below $\bar{s} = 0.5$ in Fig. S5c.

The effects of demographic stochasticity can also be seen in Fig. S5d, where the total carrying capacity K is varied (together with the time point at which coexistence is evaluated, at generation $10K$), while the strength λ of density-dependent competition and the expected survival probability $\bar{s} = K/N$ are held constant. Because we are interested in the effects of population size per se, we also hold constant the relative strength of mate-search costs ($m/K = 1$), so the ease with which females encounter preferred mates remains unaffected by changes in K. All else being equal, larger population sizes facilitate the long-term maintenance of coexisting types, as expected given the associated reduction in demographic stochasticity (the aforementioned coefficient of variation falls in proportion to $1/\sqrt{N}$).

S2.7 Altering the spatial scales of competition, mate search, and movement

In our main model, we equate the spatial scales of three processes: competition ($\sigma_s = 0.05$), mate search ($\sigma_f = 0.05$), and movement ($\sigma_m = 0.05$). Fig. S6 shows what happens when those three

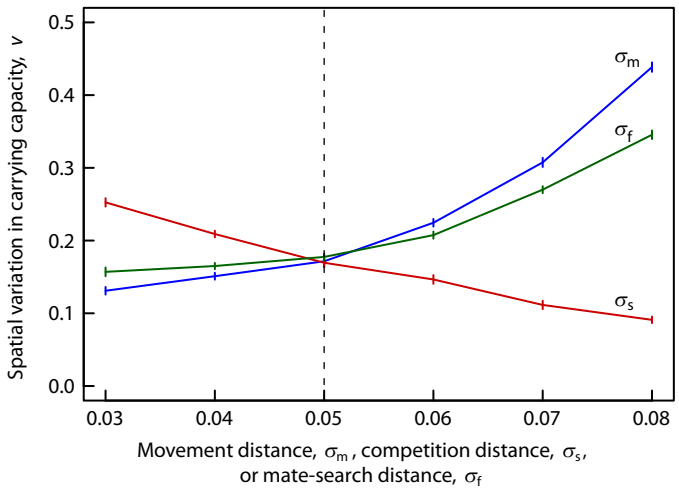

Figure S6 | Minimum level of spatial variation v in local carrying capacity needed to ensure long-term coexistence in a two-dimensional bimodal landscape. The spatial variation v is increased until the average persistence time of mating types in 20 replicate runs exceeded $10K$ generations (vertical lines indicate standard errors). The three curves show the effects of the width σ_s of the competition distribution (red), the width σ_f of the mate-search distribution (green), and the width σ_m of the movement distribution (blue), while holding all other parameters constant at their values in Fig. 1d. In the other figures, the following values (indicated by the vertical dashed line) are used: $\sigma_s = 0.05$, $\sigma_f = 0.05$, $\sigma_m = 0.05$.

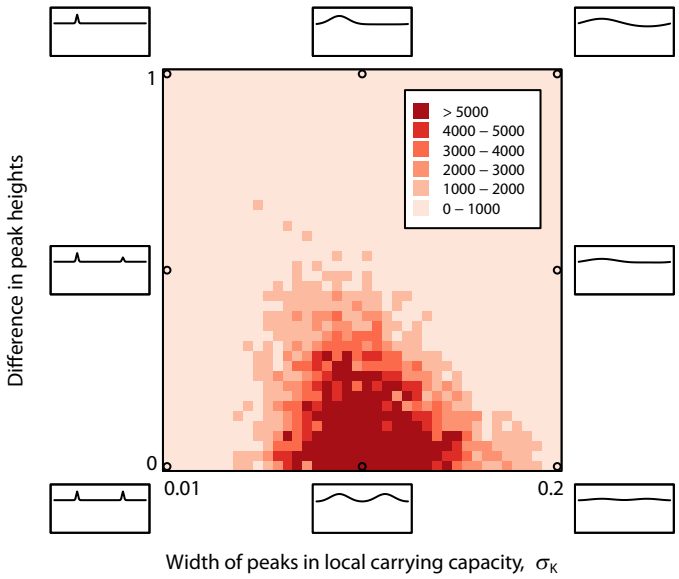

Figure S7 | Effects of altering the shape of the local carrying capacity (Eq. 1) in a two-dimensional bimodal landscape. Shading indicates how long polymorphism persists at the display locus (darker = longer). Each cell represents the mean time to loss of polymorphism for 10 replicate model runs. Side panels indicate the extent of spatial variation in local carrying capacity along transects at $y = 0.25$ for nine parameter combinations indicated by the closest open circle. The inset at the bottom center corresponds to the parameter combination used in Fig. 3. Spatial variation in local carrying capacity is relatively weak throughout this figure, with v ranging from 0.28 for $\sigma_k = 0.01$ (far left) to 0.049 for $\sigma_k = 0.2$ (far right). All other parameters are as in Fig. 1d.

spatial scales are varied independently. Coexistence is easier to maintain if female mate search and movement are more localized (smaller σ_f and smaller σ_m), because mating types predominating in different spatial regions then undergo less mixing. By contrast, coexistence is easier to maintain if competition occurs across a wider spatial range (larger σ_s), because individuals near the resource peaks

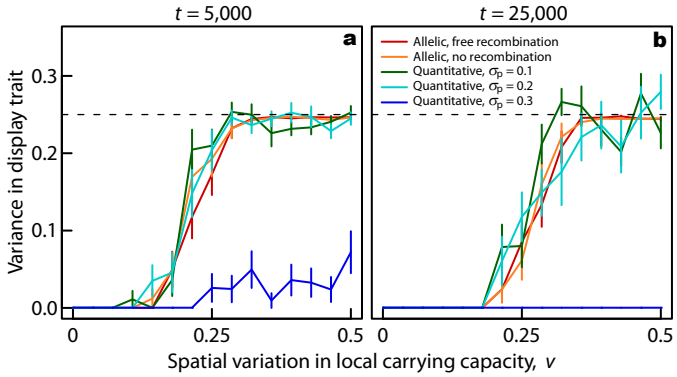

Figure S8 | Effects of changes in genetic architecture in a two-dimensional bimodal landscape. Variance in display trait after 5,000 (**a**) and 25,000 (**b**) generations for a variety of genetic architectures, averaged over 20 replicate model runs (vertical lines indicate standard errors). The dashed line indicates the maximum possible variance in the allelic model (0.25). For determining variances in the allelic model, alleles Q and q are assigned trait values 0 and 1, respectively. In the quantitative genetic model, the initial preference/display trait values are set to 0/0 or 1/1 (corresponding to P/Q or p/q in the allelic model) with equal probability, yielding an initial variance of 0.25. Over time, the variance of 0.25 can be exceeded due to random genetic drift. For comparison, the red curve shows results of our main model. Model runs are initialized as in Fig. 2. All other parameters are as in Fig. 1; in the quantitative genetic model, $\sigma_o = 0.01$.

then compete more strongly for resources in the troughs, reducing population density there and thus promoting isolation of the mating types predominating near each peak.

S2.8 Altering the shape of the local carrying capacity

We also explore the spatial scale of the resource distribution by varying the width of its peaks, as well as their relative heights, in Fig. S7. Coexistence persists as long as both peaks can maintain localized clusters of individuals.

S2.9 Incorporating alternative genetic architectures

Our main model assumes free recombination between the trait and preference loci. Fig. S8 explores the effect of linkage, finding no substantial differences between complete linkage and free recombination between the preference and display loci.

To test whether our findings are robust to changes in the number of loci, we consider a quantitative genetic model in which an individual's preference and display traits are determined by two quantitative characters. This model can be interpreted as assuming that a large (infinite) number of additive loci code for each of the two traits. Complementing our main model, which features a finite number of alleles, this extension allows for arbitrarily many mating types. In this quantitative genetic model, the probability that female i mates with male j is proportional to

$$p_{ij} = \exp(-(p_i - q_j)^2/(2\sigma_p^2))e_{ij}\,, \qquad (14)$$

where $p_i - q_j$ is the difference between the preference trait of female i and the display trait of male j, σ_p denotes the strength of female preference (smaller σ_p means females are choosier), and e_{ij} is proportional to the encounter probability between female i and male j, as defined in Eq. 7. Offspring trait values are drawn from a Gaussian function centred at the mean of the parental phenotypes for each trait, with a standard deviation σ_o that measures the variation among offspring due to segregation, recombination, and mutation. All other details of the quantitative genetic model are the same as for our main model.

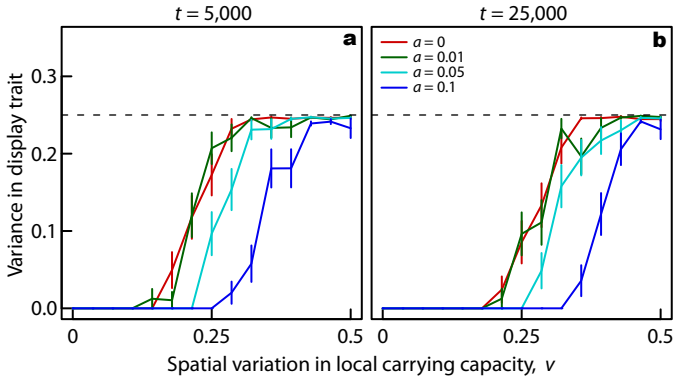

Figure S9 | Effects of asymmetric fitness costs of display traits in the allelic model in a two-dimensional bimodal landscape. Variance in display trait after 5,000 (**a**) and 25,000 (**b**) generations when males bearing the (vertical lines indicate standard errors). The dashed line indicates the maximum possible variance in this allelic model (0.25). For comparison, the red curve (identical to that in Fig. S8) shows results of our main model, corresponding to the limit $a = 0$. Model runs are initialized as in Fig. 2. All other parameters are as in Fig. 1.

Despite the different genetic assumptions, the behaviour of the quantitative genetic model closely resembles that of the allelic model (Fig. S8). Long-term coexistence of mating domains is again possible over a wide range of parameters, provided female preferences are sufficiently strong (small σ_p). As in the allelic model, loss of mating domains in the quantitative genetic model, when it happens, tends to occur through the replacement of one type by the other. Compared with the allelic model, the quantitative genetic model exhibits two additional mechanisms through which mating domains may be lost. First, when female preference is weak (large σ_p), interbreeding between adjacent mating domains may become so common that the resultant offspring form their own mating domains, facilitating the merging of the original domains. Second, the random drift of matched trait and preference values in one mating domain may cause them to coincide by chance with the values in an adjacent mating domain, so the two originally separate domains may merge due only to the random genetic drift of quantitative mating traits that results from segregation, recombination, and mutation in finite populations.

S2.10 Incorporating asymmetric display costs

Display traits can incur fitness costs in males. Our main model assumes that such costs, if present, affect all individuals equally. It may often be the case, however, that display traits differ in their effects on fitness. We therefore examine what happens when the Q allele causes males to have a reduced survival probability relative to those carrying the q allele (i.e., for Q-bearing individuals, the survival probability s_i is reduced by a factor $1 - a$, with a ranging between 0 and 1). Provided that the resultant cost is not so strong that the stabilizing effect of spatial variation in local carrying capacity is overwhelmed by selection against Q-bearing males, our main findings remain largely unchanged (Fig. S9).

27. Coulson, T., Macnulty, D. R., Stahler, D. R., Vonholdt, B., Wayne, R. K. & Smith, D. W. Modeling effects of environmental change on wolf population dynamics, trait evolution, and life history. *Science* **334**, 1275–1278 (2011).
28. Doebeli, M. & Dieckmann, U. Speciation along environmental gradients. *Nature* **421**, 259–264 (2003).